

# SafeCFG: Redirecting Harmful Classifier-Free Guidance for Safe Generation

Jiadong Pan<sup>1,2</sup> Hongcheng Gao<sup>2</sup> Liang Li<sup>1†</sup> Zheng-Jun Zha<sup>3</sup> Qingming Huang<sup>1,2</sup> Jiebo Luo<sup>4</sup>  
<sup>1</sup> Key Laboratory of Intelligent Information Processing, Institute of Computing Technology, CAS  
<sup>2</sup> University of Chinese Academy of Sciences  
<sup>3</sup> University of Science and Technology of China <sup>4</sup> University of Rochester

*WARNING: This paper contains offensive images generated by models.*



Figure 1. Generated images of SafeCFG and original CFG with increasing guidance scales, including clean images and harmful images. For clean image generation, as the guidance scale increases, SafeCFG can achieve high-quality generation similar to the original CFG. In contrast, for harmful image generation, as the guidance scale increases, SafeCFG effectively erases harmful content, which is in contrast to the original CFG, where the harmfulness of generated harmful images increases with the guidance scale.

## Abstract

Diffusion models (DMs) have demonstrated exceptional performance in text-to-image (T2I) tasks, leading to their widespread use. With the introduction of classifier-free guidance (CFG), the quality of images generated by DMs is improved. However, DMs can generate more harmful images by maliciously guiding the image generation process through CFG. Some safe guidance methods aim to mitigate the risk of generating harmful images but often reduce the quality of clean image generation. To address this issue, we introduce the **Harmful Guidance Redirector (HGR)**,

which redirects harmful CFG direction while preserving clean CFG direction during image generation, transforming CFG into SafeCFG and achieving high safety and quality generation. We train HGR to redirect multiple harmful CFG directions simultaneously, demonstrating its ability to eliminate various harmful elements while preserving high-quality generation. Additionally, we find that HGR can detect image harmfulness, allowing for unsupervised fine-tuning of safe diffusion models without pre-defined clean or harmful labels. Experimental results show that by incorporating HGR, images generated by diffusion models achieve both high quality and strong safety, and safe DMs trained through unsupervised methods according to the harmful-

<sup>†</sup>Corresponding author.

ness detected by HGR also exhibit good safety performance. The codes will be publicly available.

## 1. Introduction

In recent years, the realm of text-to-image (T2I) generation has developed rapidly, and the advancement of diffusion models (DMs) has improved both the quality of generated images and the degree of semantic matching in T2I tasks. Many high-performing DMs have been released, such as Stable Diffusion (SD) [24], Imagen [26], DALL-E-3 [2], and CogView3 [43]. By training on large-scale datasets, these models have improved image generation quality and text-image alignment ability. Classifier guidance, proposed by [4], uses classifier gradients to guide the generation process, improving diffusion model generation quality. Inspired by this, Ho and Salimans [13] proposed classifier-free guidance (CFG), which enhances the text condition for better generation quality without requiring a classifier.

Unfortunately, some malicious groups or individuals exploit DMs to generate harmful images, including nudity, violence, illegal activities, and so on [7, 23, 42]. They use CFG to direct harmful text conditioning, resulting in more harmful generated images. To address these issues, some methods [29] introduce safe guidance into image generation to avoid generating harmful content, but these approaches reduce the sample quality of clean images. Some methods [5, 10, 36] fine-tune diffusion models to make them forget harmful content at the parameter level. However, these approaches typically require datasets with pre-defined clean and harmful labels. Moreover, during the fine-tuning process, the model assigns the same safety training weight to harmful images with varying degrees of harm, making it difficult to eliminate stronger harmful concepts while also impacting the quality of clean image generation.

Previous approaches improved DM safety mainly by weakening harmful text conditions at the cost of generation quality. In fact, CFG itself can both enhance clean text conditions and weaken harmful text conditions by introducing Transformer [35] to achieve high safety and quality generation. We can leverage the Transformer’s ability to process text features, redirecting the CFG direction of harmful data and steering it toward a safe direction. Moreover, Transformer can provide a more fine-grained assessment of image harmfulness than just pre-defined harmful labels, which enables unsupervised training of safe DMs.

In this paper, we propose the **Harmful Guidance Redirector (HGR)**, a Transformer-based plug-in that can be seamlessly applied to DMs without changing the parameters of DMs, transforming CFG into SafeCFG by redirecting the CFG direction of harmful data. HGR supersedes the unconditional score estimate in CFG, preserving clean image quality with a similar score estimate for clean data and redirecting CFG to eliminate harmful content in harm-

ful images, thus transforming CFG into SafeCFG. SafeCFG enables us to achieve a DM generation process that **improves both safety and quality** simultaneously. Furthermore, HGR enables unsupervised training of safe DMs by detecting data harmfulness. Our main contributions are:

- We propose Harmful Guidance Redirector (HGR), enhancing CFG to SafeCFG by redirecting harmful CFG direction, enabling DMs to generate both high-safety and high-quality images.
- We detect the harmfulness of images and adaptively train safe DMs using HGR in an unsupervised manner without the need for predefined clean and harmful labels.
- Experimental results show that SafeCFG generates images with high safety and quality, and safe DMs by unsupervised training also show good safety performance.

## 2. Related Work

### 2.1. Text-guided Image Generation

Diffusion models (DMs) have achieved outstanding results in T2I generation, as demonstrated by models like Stable Diffusion [24], DALL-E 3 [2], and so on. In T2I scenarios, text prompts are input and processed by the text encoder, such as CLIP [22], to obtain text embeddings, which serve as conditional inputs of U-Net [25] or DiT [20] to guide the image generation process. Both U-Net and DiT utilize the cross-attention mechanism, using image embeddings as queries and text embeddings as keys and values to enhance the interaction between texts and images. Classifier-free guidance (CFG) [13] is also introduced into the text-guided image generation process. CFG enhances the text condition by combining the score estimates of conditional and unconditional generation in DMs, without the need to retrain the models. DMs generate high-quality images that closely align with input texts by leveraging CFG. We introduce Harmful Guidance Redirector (HGR) that supersedes the unconditional generation in CFG, which redirects CFG toward a safe direction when encountering harmful text embeddings and maintains CFG generation direction when facing clean text embeddings, thus achieving high quality and safety in text-guided image generation.

### 2.2. Text-to-Image Safe Diffusion Models

Initial methods enhance the safety of DMs by filtering harmful texts and images from the dataset. [2, 19, 24, 30]. These methods often require a great of time to filter images in datasets, and retraining the model consumes substantial resources and time. Some methods focus on the model rather than the dataset to prevent DMs from generating harmful images in T2I scenarios. These methods can be broadly categorized into two types: those that do not change the parameters of DMs and those that do. Some methods modify the inference process without changing the

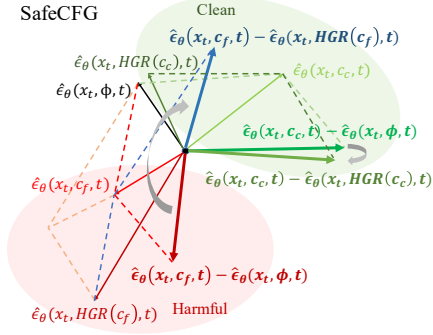


Figure 2. Illustration of SafeCFG. SafeCFG reverses the guidance direction of harmful data while preserving that of clean data, achieving high quality and safety generation. Red areas represent harmful guidance and green areas indicate clean guidance. HGR redirects harmful guidance (bold red arrow) back to clean regions (bold blue arrow) and maintains clean guidance (bold green arrow). Dashed lines show the vector addition parallelogram rule.

parameters of DMs. For instance, SLD [29] adds safe guidance to the generation process to reduce harmfulness, while UCE [6] and RECE [9] use closed-form weight editing to erase harmful concepts. Other approaches [3, 37, 38, 40] employ large language models (LLMs) or filters to remove harmful content from prompts. However, these methods often lack robustness, degrade clean image quality, or increase inference times. Some methods change the parameters of DMs to unlearn unsafe content [5, 36, 39]. ESD [5] removes harmful concepts through training DMs by negative guidance and Forget-Me-Not [39] avoids generating harmful images by eliminating attention maps associated with harmful concepts. These methods require explicit harmful labels, some cannot remove multiple harmful contents, and affect clean image generation quality. In contrast, our HGR does not change DM parameters and only needs to guide the generation process via SafeCFG, ensuring both high-quality and high-safety generation. HGR can also be extended to train-based methods for unsupervised training of DMs without the need for explicit harmful labels.

### 3. Preliminary

#### 3.1. Diffusion Models

Diffusion models (DMs) are inspired by a physical concept called non-equilibrium thermodynamics [31]. DMs, such as DDPM [14], progressively convert noise into images by using neural networks to predict noise added on images. DMs can be divided into two processes: **forward diffusion process** and **denoising process**.

**Forward diffusion process.** Given an image dataset  $D$

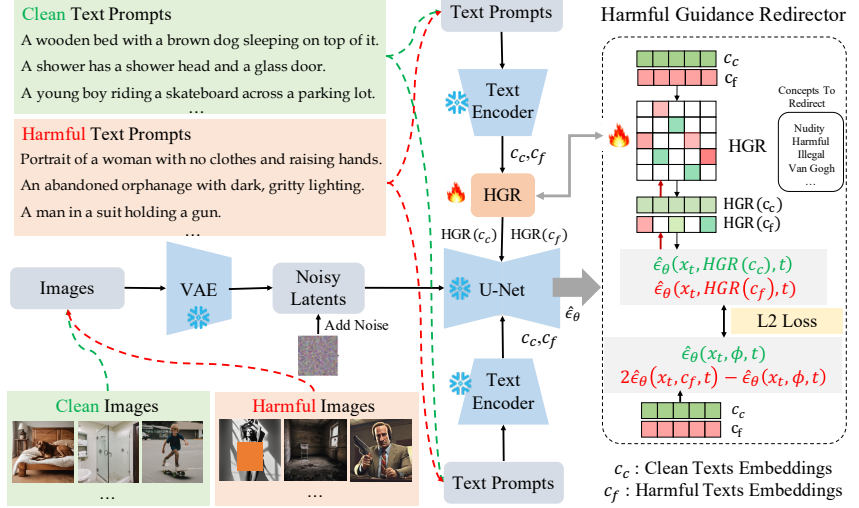


Figure 3. Training process of HGR. The prompt input provides embeddings processed with and without HGR, then predicts noise using DM. Separate noise training targets are assigned for clean data and harmful data, with HGR parameters updated based on the L2 loss of the predicted noise target. Throughout the training process, all parameters within DM remain frozen. Example clean/harmful text prompts and generated images are shown.

and the data point  $x_0 \in D$ , the forward diffusion process gradually adds a small amount of Gaussian noise on  $x_0$  in  $T$  timesteps:

$$q(\mathbf{x}_t | \mathbf{x}_{t-1}) = \mathcal{N}(\mathbf{x}_t; \sqrt{1 - \beta_t} \mathbf{x}_{t-1}, \beta_t \mathbf{I}) \quad (1)$$

where  $\mathcal{N}$  follows a normal distribution and  $\beta_t$  is a variance schedule related to  $t$ .

By using reparameterization trick [16] and let  $\alpha_t = 1 - \beta_t$  and  $\bar{\alpha}_t = \prod_{i=1}^t \alpha_i$ , we can get:

$$\mathbf{x}_t = \sqrt{\bar{\alpha}_t} \mathbf{x}_0 + \sqrt{1 - \bar{\alpha}_t} \epsilon \quad (2)$$

$\bar{\alpha}_t$  decreases as time  $t$  increases, which is close to 1 when  $t = 0$  and 0 when  $t = T$ .

**Denoising process.** The denoising process aims to predict the posterior of each forward step by a neural network  $\theta$  with time  $t$ , which makes it possible to recreate the true sample from Gaussian noise. The process can be described as:

$$p_\theta(\mathbf{x}_{t-1} | \mathbf{x}_t) = \mathcal{N}(\mathbf{x}_{t-1}; \boldsymbol{\mu}_\theta(\mathbf{x}_t, t), \boldsymbol{\Sigma}_\theta(\mathbf{x}_t, t)) \quad (3)$$

where  $\boldsymbol{\mu}_\theta(\mathbf{x}_t, t)$  and  $\boldsymbol{\Sigma}_\theta(\mathbf{x}_t, t)$  are predicted by neural network  $\theta$ . In DDPM,  $\boldsymbol{\Sigma}_\theta(\mathbf{x}_t, t)$  is set to  $\beta_t \mathbf{I}$  and  $\boldsymbol{\mu}_\theta(\mathbf{x}_t, t)$  can be derived by:

$$\boldsymbol{\mu}_\theta(\mathbf{x}_t, t) = \frac{1}{\sqrt{\alpha_t}} \left( \mathbf{x}_t - \frac{1 - \alpha_t}{\sqrt{1 - \bar{\alpha}_t}} \epsilon_\theta(\mathbf{x}_t, t) \right) \quad (4)$$

U-Net [25] or DiT [20] are trained to predict the added noise at each time step  $t$ . The noise prediction of DDPM is mathematically equivalent to score matching [32, 33]:  $\epsilon_\theta(\mathbf{x}_t, t) = -\sigma_t \nabla_{\mathbf{x}_t} \log p(\mathbf{x}_t)$ .

### 3.2. Classifier-free Guidance

Initially, DMs were trained only to estimate image distributions  $p(x_0)$ , without the ability to generate images from text prompts or labels  $c$ . To address this problem, classifier guidance (CG) [4] was introduced. CG modifies the diffusion score to include the gradient of the log-likelihood of a classifier model  $\psi$ :

$$\tilde{\epsilon}_\theta(x_t, c, t) = \epsilon_\theta(x_t, t) - \omega\sigma_t \nabla_{x_t} \log p_\psi(c|x_t) \quad (5)$$

CG requires training a classifier, which is inconvenient, and it is difficult to train such a classifier for diverse text prompts. By using Bayes' rule, it can be derived from the gradient of the log-likelihood of the classifier:

$$\begin{aligned} \nabla_{x_t} \log p_\psi(c|x_t) &= \nabla_{x_t} \log p_\psi(x_t|c) - \nabla_{x_t} \log p_\psi(x_t) \\ &= -\frac{1}{\sigma_t} (\epsilon_\theta(x_t, c, t) - \epsilon_\theta(x_t, t)) \end{aligned} \quad (6)$$

Classifier-free Guidance [13] leverages Equ.6 and substitutes Equ.6 into Equ.5, achieving a guidance way without the need for any classifier. The final score estimate of CFG derived from Equ.5 and Equ.6 is:

$$\begin{aligned} \tilde{\epsilon}_\theta(x_t, c, t) &= \epsilon_\theta(x_t, \phi, t) + (1 + \eta)(\epsilon_\theta(x_t, c, t) - \epsilon_\theta(x_t, \phi, t)) \\ &= \epsilon_\theta(x_t, c, t) + \eta(\epsilon_\theta(x_t, c, t) - \epsilon_\theta(x_t, \phi, t)) \end{aligned} \quad (7)$$

where  $\eta$  is the guidance scale, which controls the guidance degree of condition  $c$ , and  $\phi$  means no condition. In this paper, we use the Harmful Guidance Redirector (HGR) to adjust the no-condition score, keeping the score of clean data unchanged while modifying the score of harmful data to enhance safety. This operation integrates safety properties into CFG, transforming it into SafeCFG and enabling DMs to generate high-quality and high-safety images.

## 4. Methods

In this section, we present the implementation of SafeCFG using Harmful Guidance Redirector (HGR), its training method, and how HGR enables unsupervised training. Firstly, We introduced the training process of HGR and the inference process of SafeCFG in Sec. 4.1. After this, we explained how to use HGR to perform unsupervised training of safe DMs on text-image datasets in Sec. 4.2.

### 4.1. Harmful Guidance Redirector and SafeCFG

To enhance CFG [13] to SafeCFG, we introduce HGR, which is based on Transformer [35] and can be used plug-and-play on diffusion models (DMs).

Given a text-image dataset  $D$  composed of clean data  $D_c$  and harmful data  $D_f$ , where  $D_c = \{x_c^i, c_c^i\}_{i=1}^{N_c}$  and  $D_f = \{x_f^i, c_f^i\}_{i=1}^{N_f}$  and a text-to-image diffusion model  $\theta$ , which

predicts the score of the diffusion process as  $\epsilon_\theta(x_t, c, t)$ , the original CFG of both clean data and harmful data is:

$$\tilde{\epsilon}_\theta(x_t, c, t) = \epsilon_\theta(x_t, c, t) + \eta(\epsilon_\theta(x_t, c, t) - \epsilon_\theta(x_t, \phi, t)) \quad (8)$$

where text embeddings  $c$  can be  $c_c$  or  $c_f$ .

After HGR is inserted between the text encoder and the denoising architecture (U-Net or DiT), we supersede the no-condition score estimate in CFG with the score estimate from the text embedding filtered by HGR. The modified score estimate is as follows:

$$\tilde{\epsilon}_\theta(x_t, c, t) = \epsilon_\theta(x_t, c, t) + \eta(\epsilon_\theta(x_t, c, t) - \epsilon_\theta(x_t, HGR(c), t)) \quad (9)$$

The goal is: SafeCFG aligns with the original CFG for clean data, while its guidance direction opposes that of the original CFG for harmful data. The equations to achieve this are:

$$\begin{aligned} \epsilon_\theta(x_t, c_c, t) - \epsilon_\theta(x_t, HGR(c_c), t) &= \epsilon_\theta(x_t, c_c, t) - \epsilon_\theta(x_t, \phi, t) \\ \epsilon_\theta(x_t, c_f, t) - \epsilon_\theta(x_t, HGR(c_f), t) &= -(\epsilon_\theta(x_t, c_f, t) - \epsilon_\theta(x_t, \phi, t)) \end{aligned} \quad (10)$$

It can solved as:

$$\begin{aligned} \epsilon_\theta(x_t, HGR(c_c), t) &= \epsilon_\theta(x_t, \phi, t) \\ \epsilon_\theta(x_t, HGR(c_f), t) &= 2\epsilon_\theta(x_t, c_f, t) - \epsilon_\theta(x_t, \phi, t) \end{aligned} \quad (11)$$

We make HGR trainable while keeping the other structures frozen during the training process of HGR. The training objective is to use L2 loss to bring the score estimate of HGR  $\epsilon_\theta(x_t, HGR(c), t)$  close to the target specified in Equ.11. Fig. 3 shows the training process of HGR.

The training objective can also be explained from the perspective of possibility. It decreases the likelihood of harmful data and improves the likelihood of clean data. See Appendix 7 for a detailed proof.

Replacing the unconditional score estimation  $\epsilon_\theta(x_t, \phi, t)$  with the score after filtering through HGR offers two key benefits: for clean data, HGR yields a score similar to the unconditional score estimate, while for harmful data, it provides a safety-optimized filtered score. Compared to filtering all text embeddings  $c$ , this approach is easier to train and preserves the conditional score estimation  $\epsilon_\theta(x_t, c, t)$ , ensuring both safety and quality. Additionally, the Transformer-based HGR harnesses its ability to process text features, effectively filtering diverse harmful data.

The inference process of SafeCFG during image generation is as follows:

$$\tilde{\epsilon}_\theta(x_t, c, t) = \epsilon_\theta(x_t, c, t) + \eta(\epsilon_\theta(x_t, c, t) - \epsilon_\theta(x_t, HGR(c), t)) \quad (12)$$

There is no longer a need to distinguish whether the text prompts are harmful. Fig. 2 illustrates that SafeCFG changes the guidance direction of harmful data while retaining that of clean data, enabling high-quality and high-safety generation.

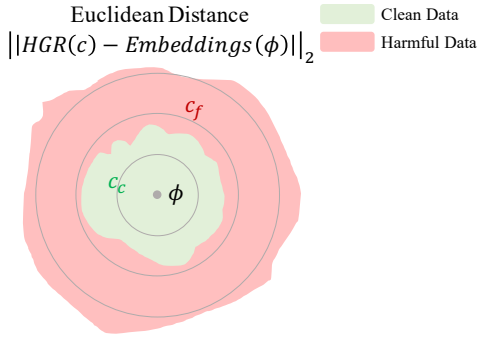


Figure 4. Illustration of HGR properties.  $HGR(c)$  for clean data is closer to  $\text{Embeddings}(\phi)$  than for harmful data, supporting HGR as an unsupervised method for training a safe model.

Fig. 1 shows examples of SafeCFG and original CFG. Compared with the original CFG, SafeCFG achieves both high-safety and high-quality generation.

## 4.2. Unsupervised Training of Safe DMs

In Sec. 4.1, we introduce HGR and SafeCFG. As HGR makes different score estimates for clean and harmful data, it is possible to leverage HGR for unsupervised training of safe DMs.

HGR gives different score estimates for clean data and harmful data:

$$\begin{aligned} \epsilon_{\theta}(x_t, HGR(c_c), t) &\approx \epsilon_{\theta}(x_t, \phi, t) \\ \epsilon_{\theta}(x_t, HGR(c_f), t) &\approx 2\epsilon_{\theta}(x_t, c_f, t) - \epsilon_{\theta}(x_t, \phi, t) \end{aligned} \quad (13)$$

It makes  $HGR(c_c)$  closer to  $\phi$  than  $HGR(c_f)$ , which means that the distance between  $HGR(c)$  and  $\phi$  can be a symbol of the harmfulness of text embedding  $c$ . The property of the HGR is illustrated in Fig. 4. We leverage the above properties of HGR to dynamically train safe DMs in an unsupervised fashion.

Fig. 5 illustrates the unsupervised training process. Given a text-image dataset  $D = \{x^i, c^i\}_{i=1}^N$ , which contains both clean and harmful data without any label, and two instances of DMs:  $\theta$  and  $\theta^*$ , where  $\theta$  is frozen and  $\theta^*$  is trainable, we use HGR firstly to calculate the euclidean distance between  $HGR(c)$  and  $\phi$ :

$$dis(c) = ||HGR(c) - \text{Embeddings}(\phi)||_2 \quad (14)$$

where  $\text{Embeddings}$  means text embeddings using Text Encoder to encode  $\phi$  prompt. As the distance is the symbol of the harmfulness of  $c$ , we set the threshold distance  $dis_t$ . When  $dis(c)$  is large than  $dis_t$ , the score estimate of  $\theta^*$  on  $c$   $\epsilon_{\theta^*}(x_t, c, t)$  is trained towards a safe direction. The training

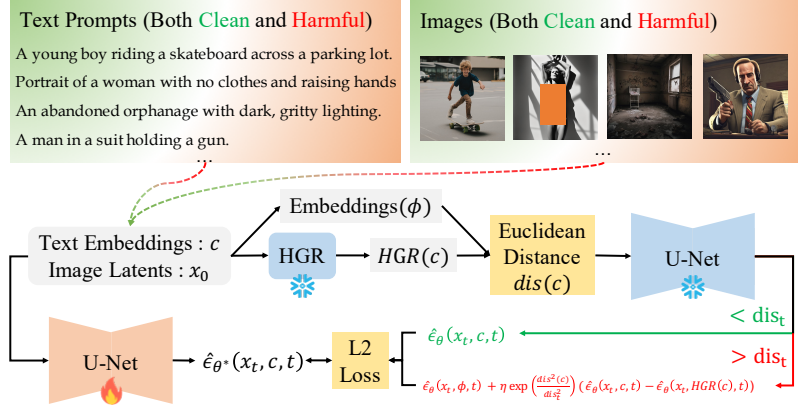


Figure 5. Unsupervised training process. Given text embeddings  $c$  and image latent  $x_0$ , we use two DMs: one frozen and one trainable. HGR calculates  $dis(c)$  as an indicator of  $c$ 's harmfulness to guide training direction, dynamically updating the trainable DM's parameters based on  $c$ 's harmfulness.

objective is:

$$\begin{aligned} \epsilon_{\theta^*}(x_t, c, t) &\leftarrow \epsilon_{\theta}(x_t, c, t) & , dis(c) \leq dis_t \\ \epsilon_{\theta^*}(x_t, c, t) &\leftarrow \epsilon_{\theta}(x_t, \phi, t) + \eta \exp\left(\frac{dis^2(c)}{dis_t^2}\right) (\epsilon_{\theta}(x_t, c, t) - \epsilon_{\theta}(x_t, HGR(c), t)) & , dis(c) > dis_t \end{aligned} \quad (15)$$

where  $\eta$  controls the degree of safe guidance and  $\exp\left(\frac{dis^2(c)}{dis_t^2}\right)$  dynamically changing according to the harmfulness of text embedding  $c$ . Finally, DM  $\theta^*$  becomes safe DM trained by an unsupervised training method.

## 5. Experiments

We conduct comprehensive experiments to evaluate the performance of our method. In Sec. 5.2, we demonstrate that Harmful Guidance Redirector (HGR) and SafeCFG enable diffusion models (DMs) to generate high-quality images while removing harmful content. In Sec. 5.3, we demonstrate that DMs fine-tuned using the unsupervised training method can also show good safety performance. We also do art-style erasing experiments, which show the ability of our models to erase different kinds of concepts simultaneously.

### 5.1. Experimental Setup

**Datasets.** We sample text prompts from Laion-5B [30] and COCO [18], and generate images with Stable Diffusion (SD) [24] to create a clean text-image dataset. We sample text prompts from I2P [29], generate harmful prompts using Mistral-7B [15], and create images with SD to form a harmful text-image dataset. In art style erasing experiments, we focus on removing the styles of Van Gogh and Picasso while preserving those of 25 other artists, using prompts for Van Gogh, Picasso, and generic artists [5].

**Models.** Stable Diffusion models [24] are popular open-resource T2I models. We train the Harmful Guidance Redirector (HGR) and apply SafeCFG on SD V1.4, V2.1, and SD XL [21]. Due to high memory demands, unsupervised

Evaluation Type	Nudity		Illegal		Violence		Clean							
	CFG	SafeCFG	CFG	SafeCFG	CFG	SafeCFG	CFG	SafeCFG	CFG	SafeCFG	CFG	SafeCFG		
Guidance Scale	NudeNet ↓		Q16-illegal ↓		Q16-violence ↓		FID ↓		IS ↑		CLIP Score ↑		Aesthetic Score ↑	
0	0.11	0.11	0.29	0.29	0.39	0.39	30.34	30.34	22.91	22.91	0.41	0.41	5.79	5.79
1.5	0.31	0.11	0.35	0.24	0.43	0.31	9.31	9.41	37.07	36.90	0.39	0.40	6.10	6.11
3.0	0.53	0.06	0.34	0.17	0.44	0.24	9.80	9.88	40.56	40.46	0.39	0.39	6.19	6.20
4.5	0.51	0.07	0.33	0.12	0.43	0.20	11.37	11.72	41.25	41.05	0.39	0.39	6.24	6.25
6.0	0.56	0.05	0.35	0.11	0.44	0.19	12.89	13.30	41.42	41.07	0.39	0.39	6.26	6.26
7.5	0.61	0.04	0.36	0.10	0.45	0.14	14.16	14.60	41.43	41.79	0.39	0.39	6.26	6.27
9.0	0.60	<b>0.04</b>	0.37	<b>0.09</b>	0.45	<b>0.12</b>	15.48	15.66	42.57	42.36	0.39	0.39	6.28	6.27

Table 1. Comparison of safety between SafeCFG and original CFG shows that SafeCFG generates increasingly safer images with higher guidance scales, while CFG produces more harmful images under the same conditions. In terms of generation quality, SafeCFG maintains performance similar to the original CFG, with comparable FID, IS, CLIP Score and Aesthetic Score.

fine-tuning of safe DMs was only conducted on SD V1.4 and V2.1.

**Metrics.** We include metrics to evaluate the safety and the generation quality of DMs. To evaluate the safety of DMs on I2P [29], we use **NudeNet** [1] and **Q16** [28]. NudeNet is efficient in detecting sexual content in images and Q16 can detect other types of harmful content, such as violent and illegal images. To evaluate the generation quality of DMs on COCO-30K [18], we use **Fréchet Inception Distance (FID)** [12], **CLIP Score (CS)** [11] and **Aesthetic Score (AS)** [17]. FID correlates well with human judgments of visual quality and is a useful metric for evaluating generation quality. CLIP Score assesses the alignment between generated images and their corresponding text prompts. Aesthetic Score is calculated by part of CLIP [22] to evaluate the aesthetic quality of images. To evaluate the performance of art-style erasing experiments, we measure the **Learned Perceptual Image Patch Similarity (LPIPS)** [41] and **Style Loss (SL)** [8] between the unedited and edited images.

**Configurations.** HGR is based on a Transformer with 2 layers and 16 attention heads. Its hidden dimension matches the text embeddings from the corresponding DM version: 768 for SD V1.4, 1024 for SD V2.1, and 2048 for SD XL.

## 5.2. Performance of SafeCFG

We evaluate our SafeCFG in terms of safety performance and generation quality, while also assessing its performance in erasing art style.

### 5.2.1. Quantitative Results

The quantitative results related to the safety of generated harmful images and the quality of generated clean images are shown in Table 2. Compared to other safety methods for DMs, SafeCFG by HGR achieves high-quality, safe generation with lower harmful concept detection (NudeNet, Q16), lower FID, similar CLIP Score, and higher Aesthetic Score. Visual examples in Fig. 6 and Appendix 8 show that SafeCFG generates both high-safety and high-quality images.

Evaluation Type	Sexual	Illegal	Violence	Clean		
	NudeNet ↓	Q16-i ↓	Q16-v ↓	FID ↓	CS ↑	AS ↑
SD V1.4	0.61	0.36	0.46	14.16	0.39	6.26
ESD-Nudity-u1 [5]	0.16	0.33	0.37	<u>14.69</u>	0.38	<u>6.24</u>
ESD-Nudity-u3 [5]	0.12	0.19	0.34	19.74	0.39	6.04
ESD-Nusity-u10 [5]	0.08	0.16	0.26	23.67	0.39	6.01
ESD-Violence-u1 [5]	0.48	0.19	0.27	16.51	0.39	6.15
ESD-Illegal-u1 [5]	0.45	0.29	0.39	16.33	0.39	6.17
SA [10]	0.08	0.13	<b>0.11</b>	28.13	0.38	5.95
UCE [6]	0.20	0.20	0.33	16.59	0.39	6.16
RECE [9]	0.09	0.14	0.19	18.46	0.39	6.07
SLD-Weak [29]	0.23	0.25	0.36	15.89	0.39	6.16
SLD-Medium [29]	0.14	0.19	0.23	17.06	0.40	6.13
SLD-Strong [29]	0.09	<u>0.10</u>	0.17	19.14	0.39	6.06
SLD-Max [29]	<u>0.06</u>	<b>0.06</b>	<u>0.14</u>	21.03	0.40	6.02
SD V1.4+HGR (Ours)	<b>0.04</b>	<u>0.10</u>	<u>0.14</u>	<b>14.60</b>	0.39	<b>6.27</b>
SD V2.1	0.36	0.31	0.43	16.81	0.40	6.14
SD V2.1+HGR (Ours)	0.02	0.04	0.05	18.38	0.40	6.11
SD XL	0.41	0.31	0.38	14.82	0.39	6.26
SD XL+HGR (Ours)	0.01	0.09	0.09	15.34	0.39	6.28

Table 2. Quantitative results on the safety of generated harmful images and the quality of clean images show that our method outperforms others in FID and Aesthetic Score, indicating it maintains high quality in generated clean images. We also rank highly in the NudeNet and Q16 metrics, demonstrating effective safety enhancement. The **bold** indicates the best performance, while the underline indicates the second-best. Q16-i refers to Q16-illegal, Q16-v to Q16-violence, CS to CLIP Score, and AS to Aesthetic Score. The guidance scale is set to 7.5 during generation.

### 5.2.2. Different Guidance Scale

We set different safe guidance scales for SafeCFG and evaluated the safety of harmful images and the quality of clean images. Visual images are shown in Fig. 1 and Appendix 9. The quantitative results are shown in Table 1. We also evaluate the Inception Score (IS) [27] on clean images here following the evaluation metrics used in [13].

Compared to the original CFG, SafeCFG significantly improves safety. The original CFG produces increasingly harmful images as the guidance scale increases. In contrast, SafeCFG achieves the opposite effect, generating images that become less harmful with a higher guidance scale, which is evidenced by the progressively lower ratios of harmful content detected by NudeNet and Q16 as the guidance scale increases in SafeCFG.

SafeCFG maintains a similar image quality to the original CFG for clean images. As the guidance scale increases, FID rises, IS increases, CLIP Score stays the same, and Aesthetic Score improves. These trends align with findings

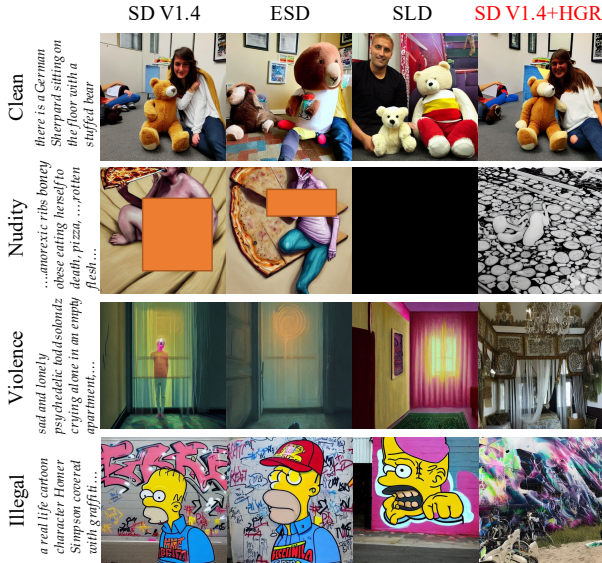


Figure 6. Images generated by different safe methods. Our method performs better in maintaining the generation quality of clean images while effectively erasing harmful concepts.

Art Style	Van Gogh		Picasso		Generic Artists	
	LPIPS $\uparrow$	SL $\uparrow$	LPIPS $\uparrow$	SL $\uparrow$	LPIPS $\downarrow$	SL $\downarrow$
ESD-x-1 [5]	0.368	0.025	0.204	0.004	0.227	0.018
SLD-Medium [29]	0.275	0.013	0.201	0.003	<b>0.178</b>	<b>0.006</b>
UCE [6]	0.298	0.016	0.218	0.005	0.204	0.015
RECE [9]	0.316	0.019	0.228	0.011	0.209	0.017
SD V1.4+HGR	<u>0.525</u>	<u>0.036</u>	<u>0.497</u>	<u>0.105</u>	0.341	0.068
SD V2.1+HGR	0.463	0.029	0.464	0.046	0.340	0.030
SD XL+HGR	<b>0.568</b>	<b>0.042</b>	<b>0.510</b>	<b>0.114</b>	0.329	0.010

Table 3. Results show our method effectively erases Van Gogh’s and Picasso’s art styles simultaneously, better than others, though it slightly affects other styles. The **bold** indicates the best performance, while the underline indicates the second-best. SL refers to Style Loss. The guidance scale is set to 7.5 during generation.

Art Style	Van Gogh		Picasso		Generic Artists	
	LPIPS $\uparrow$	SL $\uparrow$	LPIPS $\uparrow$	SL $\uparrow$	LPIPS $\downarrow$	SL $\downarrow$
GS						
0	0.397	0.023	0.325	0.013	0.269	0.021
1.5	0.448	0.028	0.370	0.026	0.286	0.028
3.0	0.476	0.030	0.418	0.043	0.304	0.040
4.5	0.495	0.032	0.453	0.072	0.320	0.049
6.0	0.512	0.033	0.478	0.092	0.333	0.052
7.5	0.525	0.036	0.497	0.105	0.341	0.068
9.0	0.537	0.040	0.509	0.151	0.348	0.075

Table 4. Results show that as the safe guidance scale increases, the model’s ability to remove Van Gogh’s and Picasso’s artistic styles improves. GS refers to guidance scale, and SL means Style Loss.

in [13], showing that SafeCFG preserves image generation quality while enhancing safety.

### 5.2.3. Removal of Artistic Styles

To demonstrate the versatility, we use the same HGR to simultaneously remove both art styles and harmful concepts. Table 3 shows the results of removing Van Gogh’s and Picasso’s styles, where our method outperforms others in both cases. The results show that HGR simultaneously erases

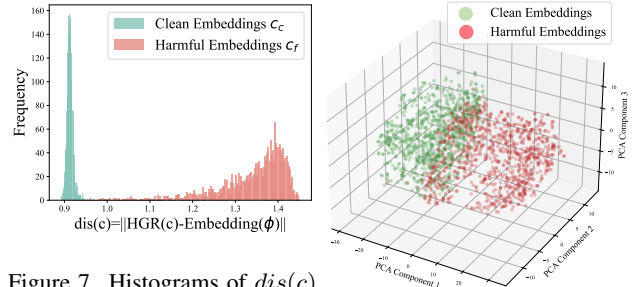


Figure 7. Histograms of  $dis(c)$  for clean and harmful concepts

show that  $dis(c)$  enables un- Figure 8. Using t-SNE to visualize supervised training. This distance also measures the harm- of clean and harmful concepts, fulness of  $c$ , aiding in the dy- which occupy different posi- namic adjustment of parameters tions in the text embedding for safety-aligned training. space.

different art styles, achieving high LPIPS and Style Loss for both Van Gogh and Picasso. However, LPIPS and Style Loss are slightly higher for generic artists, likely due to the simultaneous removal of multiple concepts. We also provide generated images of Van Gogh’s concept removal in Fig. 9 to demonstrate the effectiveness of our method.

We assess the impact of the SafeCFG guidance scale on removing artistic styles. As shown in Table 4, as the safe guidance scale increases, the model’s ability to remove the concepts of Van Gogh and Picasso strengthens. This finding is consistent with the safe guidance scale’s effect on removing harmful concepts.

## 5.3. Unsupervised Training by Leveraging HGR

First, we visualize the performance of assessing the harmfulness of  $c$  by measuring the distance between  $HGR(c)$  and  $Embeddings(\phi)$ . Then, we evaluated the safety performance and generation quality of the safe model trained by the unsupervised approach. Additionally, we assessed the performance of the unsupervised training method in simultaneously erasing art style and harmful concepts.

### 5.3.1. Visualization of HGR’s Ability to Distinguish Different Concepts

In Sec. 4.2, we analyze that the distance between  $HGR(c)$  and  $\phi$  can be a measurement of the harmfulness of text embedding  $c$ . We randomly select 2,000 clean prompts and 2,000 harmful prompts, calculate their distribution based on  $dis(c)$ , and plot histograms of  $dis(c)$  for clean and harmful concepts. The results are shown in the Fig. 7. The  $dis(c)$  of clean embeddings is around 0.9 and that of harmful embeddings  $c_f$  is larger. The difference in distance between harmful embeddings and clean embeddings from  $Embeddings(\phi)$  enables unsupervised training. Additionally, this distance difference can measure the harmfulness of  $c$ , supporting the dynamic adjustment of degree for safety-aligned training.

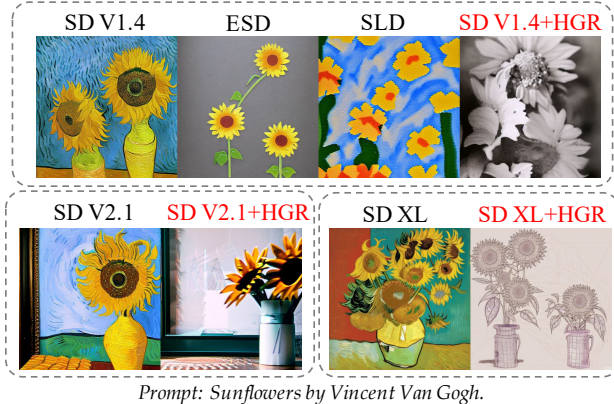


Figure 9. Generated images removing Van Gogh’s styles. Our models remove Van Gogh’s styles more thoroughly.

Evaluation Type	Sexual			Clean		
	NudeNet ↓	Q16-i ↓	Q16-v ↓	FID ↓	CLIP S ↑	AS ↑
SD V1.4	0.61	0.36	0.46	14.16	0.39	6.26
ESD-Nudity-u1 [5]	0.16	0.33	0.37	<b>14.69</b>	0.38	6.24
ESD-Nudity-u3 [5]	0.12	0.19	0.34	19.74	0.39	6.04
ESD-Nudity-u10 [5]	0.08	0.16	0.26	23.67	0.39	6.01
ESD-Violence-u1 [5]	0.48	<b>0.19</b>	<b>0.27</b>	16.51	0.39	6.15
ESD-Illegal-u1 [5]	0.45	0.29	0.39	<u>16.33</u>	0.39	6.17
UT (SD V1.4, Ours)	<b>0.09</b>	<b>0.23</b>	<b>0.32</b>	19.16	0.39	6.13
SD V2.1	0.36	0.31	0.43	16.81	0.40	6.14
UT (SD V2.1, Ours)	0.11	0.27	0.38	21.12	0.40	6.01

Table 5. Results of our unsupervised trained safe model. Compared to ESD, our model shows similar or better safety performance and improved clean image quality under comparable conditions (ESD-u3). The **bold** indicates the best performance, and the underline indicates the second-best. UT refers to unsupervised training, Q16-i to Q16-illegal, Q16-v refers to Q16-violence, CLIP S to CLIP Score, and AS refers to Aesthetic Score.

In addition, we use t-SNE [34] to visualize  $HGR(c)$  – Embeddings( $\phi$ ) of clean and harmful concepts. The results are shown in Fig. 8.  $HGR(c)$  – Embeddings( $\phi$ ) for clean and harmful types occupy different positions in the text embedding space, highlighting HGR’s ability to distinguish between concepts and enabling high-quality and high-safety generation.

### 5.3.2. Quantitative Results

We evaluated our unsupervised safe model for safety and generation quality, as shown in Table 5. Compared to ESD, our model achieved similar or better safety performance and improved clean image quality under comparable conditions (ESD-u3). This may be due to the dynamic safe guidance degree in our unsupervised training, which has less impact on clean images but a greater effect on harmful ones.

### 5.3.3. Different Guidance Scale and Training Steps

We conducted some ablation experiments on the number of training steps and the guidance degree  $\eta$ , which are shown in Appendix 10. The experimental results indicate that as the number of training steps and  $\eta$  increase, the model becomes increasingly safe but at the cost of generation quality.

Art Style	Van Gogh		Picasso		Generic Artists	
	LPIPS ↑	SL ↑	LPIPS ↑	SL ↑	LPIPS ↓	SL ↓
ESD-x-1 [5]	<b>0.368</b>	<b>0.025</b>	0.204	0.004	0.227	0.018
SLD-Medium [29]	0.275	0.013	0.201	0.003	<b>0.178</b>	<b>0.006</b>
UCE [6]	0.298	0.016	0.218	0.005	<u>0.204</u>	<u>0.015</u>
RECE [9]	0.316	0.019	<u>0.228</u>	<u>0.011</u>	0.209	0.017
UT (Ours)	<u>0.338</u>	<u>0.020</u>	<b>0.232</b>	<b>0.013</b>	0.223	0.020

Table 6. Results show that our unsupervised method can erase art styles. The **bold** font indicates the best performance, and the underline mark indicates the second-best. UT refers to unsupervised training, and SL means Style Loss.

### 5.3.4. Unsupervised Removal of Artistic Styles

We also attempt to simultaneously remove artistic styles and harmful concepts from the model trained in an unsupervised manner. The results are shown in Table 6. Compared to ESD-Vangogh-x1, our approach effectively removes both Van Gogh and Picasso styles while better preserving generic artist concepts, demonstrating the ability of our unsupervised method to erase art styles.

Furthermore, we also evaluate the effect of  $\eta$  in Eq. 15 and training steps on the removal of art styles, which are shown in Appendix 11. It can be observed that a larger  $\eta$  and more training steps result in a greater degree of removal of artistic styles.

## 5.4. Limitations and Future Work

We demonstrate unsupervised training of safe image generation models. Although our unsupervised training approach improves generation quality compared to the previous safe methods, the quality still falls short of that of the original DMs when parameters are altered. Improving both quality and safety in parameter-modified safe DMs is essential for commercially viable open-source models. Additionally, we reverse the entire harmful text’s CFG direction in HGR, which is an easy-to-operate method. However, this approach lacks good controllability over harmful image generation. In the future, we will explore revising the CFG direction of harmful parts of harmful prompts by fine-grained training on HGR to achieve better image generation controllability for harmful prompts.

## 6. Conclusion

This paper presents the Harmful Guidance Redirector (HGR) that can be used in a plug-and-play fashion with diffusion models (DMs), thus enabling safe Classifier-free Guidance (CFG) in text-to-image generation. Experimental results show that our SafeCFG enables both high-quality and high-safety generation of DMs, erasing harmful concepts and generating high-quality clean images. Moreover, HGR can be used for unsupervised training of safe DMs. Experimental results indicate the high safety of safe DMs trained in an unsupervised manner. We also show that SafeCFG can erase art styles, which demonstrates the versatility of our method.



## References

- [1] P Bedapudi. Nudenet: Neural nets for nudity classification, detection and selective censoring, 2019. 6
- [2] James Betker, Gabriel Goh, Li Jing, Tim Brooks, Jianfeng Wang, Linjie Li, Long Ouyang, Juntang Zhuang, Joyce Lee, Yufei Guo, et al. Improving image generation with better captions. *Computer Science*. <https://cdn.openai.com/papers/dall-e-3.pdf>, 2(3):8, 2023. 2
- [3] Yuzhu Cai, Sheng Yin, Yuxi Wei, Chenxin Xu, Weibo Mao, Felix Juefei-Xu, Siheng Chen, and Yanfeng Wang. Ethical-lens: Curbing malicious usages of open-source text-to-image models. *arXiv preprint arXiv:2404.12104*, 2024. 3
- [4] Prafulla Dhariwal and Alexander Nichol. Diffusion models beat gans on image synthesis. In *Advances in Neural Information Processing Systems*, 2021. 2, 4
- [5] Rohit Gandikota, Joanna Materzynska, Jaden Fiotto-Kaufman, and David Bau. Erasing concepts from diffusion models. In *Proceedings of the IEEE/CVF International Conference on Computer Vision, ICCV*, pages 2426–2436, 2023. 2, 3, 5, 6, 7, 8
- [6] Rohit Gandikota, Hadas Orgad, Yonatan Belinkov, Joanna Materzyńska, and David Bau. Unified concept editing in diffusion models. In *Proceedings of the IEEE/CVF Winter Conference on Applications of Computer Vision*, pages 5111–5120, 2024. 3, 6, 7, 8
- [7] Hongcheng Gao, Hao Zhang, Yinpeng Dong, and Zhi-jie Deng. Evaluating the robustness of text-to-image diffusion models against real-world attacks. *arXiv preprint arXiv:2306.13103*, 2023. 2
- [8] Leon A Gatys, Alexander S Ecker, and Matthias Bethge. Image style transfer using convolutional neural networks. In *Proceedings of the IEEE conference on computer vision and pattern recognition*, pages 2414–2423, 2016. 6
- [9] Chao Gong, Kai Chen, Zhipeng Wei, Jingjing Chen, and Yungang Jiang. Reliable and efficient concept erasure of text-to-image diffusion models. *arXiv preprint arXiv:2407.12383*, 2024. 3, 6, 7, 8
- [10] Alvin Heng and Harold Soh. Selective amnesia: A continual learning approach to forgetting in deep generative models. *Advances in Neural Information Processing Systems*, 36, 2024. 2, 6
- [11] Jack Hessel, Ari Holtzman, Maxwell Forbes, Ronan Le Bras, and Yejin Choi. Clipscore: A reference-free evaluation metric for image captioning, 2022. 6
- [12] Martin Heusel, Hubert Ramsauer, Thomas Unterthiner, Bernhard Nessler, and Sepp Hochreiter. Gans trained by a two time-scale update rule converge to a local nash equilibrium. In *Advances in Neural Information Processing Systems*, pages 6626–6637, 2017. 6
- [13] Jonathan Ho and Tim Salimans. Classifier-free diffusion guidance. *arXiv preprint arXiv:2207.12598*, 2022. 2, 4, 6, 7
- [14] Jonathan Ho, Ajay Jain, and Pieter Abbeel. Denoising diffusion probabilistic models. In *Advances in Neural Information Processing Systems*, 2020. 3
- [15] Albert Q Jiang, Alexandre Sablayrolles, Arthur Mensch, Chris Bamford, Devendra Singh Chaplot, Diego de las Casas, Florian Bressand, Gianna Lengyel, Guillaume Lample, Lucile Saulnier, et al. Mistral 7b. *arXiv preprint arXiv:2310.06825*, 2023. 5
- [16] Durk P Kingma, Tim Salimans, and Max Welling. Variational dropout and the local reparameterization trick. *Advances in Neural Information Processing Systems*, 28, 2015. 3
- [17] LAION-AI. Laion-aesthetics-predictor v1. <https://github.com/LAION-AI/aesthetic-predictor>, 2022. 6
- [18] Tsung-Yi Lin, Michael Maire, Serge Belongie, James Hays, Pietro Perona, Deva Ramanan, Piotr Dollár, and C Lawrence Zitnick. Microsoft coco: Common objects in context. In *Computer Vision—ECCV 2014: 13th European Conference, Zurich, Switzerland, September 6–12, 2014, Proceedings, Part V 13*, pages 740–755. Springer, 2014. 5, 6
- [19] Alex Nichol, Prafulla Dhariwal, Aditya Ramesh, Pranav Shyam, Pamela Mishkin, Bob McGrew, Ilya Sutskever, and Mark Chen. Glide: Towards photorealistic image generation and editing with text-guided diffusion models. *arXiv preprint arXiv:2112.10741*, 2021. 2
- [20] William Peebles and Saining Xie. Scalable diffusion models with transformers. In *Proceedings of the IEEE/CVF International Conference on Computer Vision*, pages 4195–4205, 2023. 2, 3
- [21] Dustin Podell, Zion English, Kyle Lacey, Andreas Blattmann, Tim Dockhorn, Jonas Müller, Joe Penna, and Robin Rombach. Sdxl: Improving latent diffusion models for high-resolution image synthesis. *arXiv preprint arXiv:2307.01952*, 2023. 5
- [22] Alec Radford, Jong Wook Kim, Chris Hallacy, Aditya Ramesh, Gabriel Goh, Sandhini Agarwal, Girish Sastry, Amanda Askell, Pamela Mishkin, Jack Clark, et al. Learning transferable visual models from natural language supervision. In *International Conference on Machine Learning*, pages 8748–8763. PMLR, 2021. 2, 6
- [23] Javier Rando, Daniel Paleka, David Lindner, Lennart Heim, and Florian Tramèr. Red-teaming the stable diffusion safety filter. *arXiv preprint arXiv:2210.04610*, 2022. 2
- [24] Robin Rombach, Andreas Blattmann, Dominik Lorenz, Patrick Esser, and Björn Ommer. High-resolution image synthesis with latent diffusion models. In *Proceedings of the IEEE/CVF conference on computer vision and pattern recognition*, pages 10684–10695, 2022. 2, 5
- [25] Olaf Ronneberger, Philipp Fischer, and Thomas Brox. U-net: Convolutional networks for biomedical image segmentation. In *International Conference on Medical image computing and computer-assisted intervention*, pages 234–241. Springer, 2015. 2, 3
- [26] Chitwan Saharia, William Chan, Saurabh Saxena, Lala Li, Jay Whang, Emily L Denton, Kamyar Ghasemipour, Raphael Gontijo Lopes, Burcu Karagol Ayan, Tim Salimans, et al. Photorealistic text-to-image diffusion models with deep language understanding. In *Advances in Neural Information Processing Systems*, pages 36479–36494, 2022. 2
- [27] Tim Salimans, Ian Goodfellow, Wojciech Zaremba, Vicki Cheung, Alec Radford, and Xi Chen. Improved techniques

- for training gans. In *Advances in Neural Information Processing Systems*, 2016. 6
- [28] Patrick Schramowski, Christopher Tauchmann, and Kristian Kersting. Can machines help us answering question 16 in datasheets, and in turn reflecting on inappropriate content? In *Proceedings of the 2022 ACM Conference on Fairness, Accountability, and Transparency*, pages 1350–1361, 2022. 6
- [29] Patrick Schramowski, Manuel Brack, Björn Deiseroth, and Kristian Kersting. Safe latent diffusion: Mitigating inappropriate degeneration in diffusion models. In *Proceedings of the IEEE/CVF Conference on Computer Vision and Pattern Recognition*, pages 22522–22531, 2023. 2, 3, 5, 6, 7, 8
- [30] Christoph Schuhmann, Romain Beaumont, Richard Vencu, Cade Gordon, Ross Wightman, Mehdi Cherti, Theo Coombes, Aarush Katta, Clayton Mullis, Mitchell Wortsman, Patrick Schramowski, Srivatsa Kundurthy, Katherine Crowson, Ludwig Schmidt, Robert Kaczmarczyk, and Jenia Jitsev. Laion-5b: An open large-scale dataset for training next generation image-text models, 2022. 2, 5
- [31] Jascha Sohl-Dickstein, Eric Weiss, Niru Maheswaranathan, and Surya Ganguli. Deep unsupervised learning using nonequilibrium thermodynamics. In *International Conference on Machine Learning*, pages 2256–2265. PMLR, 2015. 3
- [32] Yang Song and Stefano Ermon. Generative modeling by estimating gradients of the data distribution. In *Advances in Neural Information Processing Systems*, pages 11895–11907, 2019. 3
- [33] Yang Song, Jascha Sohl-Dickstein, Diederik P Kingma, Abhishek Kumar, Stefano Ermon, and Ben Poole. Score-based generative modeling through stochastic differential equations. In *International Conference on Learning Representations*, 2021. 3
- [34] Laurens Van der Maaten and Geoffrey Hinton. Visualizing data using t-sne. *Journal of machine learning research*, 9 (11), 2008. 8
- [35] A Vaswani. Attention is all you need. *Advances in Neural Information Processing Systems*, 2017. 2, 4
- [36] Jing Wu, Trung Le, Munawar Hayat, and Mehrtash Harandi. Erasediff: Erasing data influence in diffusion models. *arXiv preprint arXiv:2401.05779*, 2024. 2, 3
- [37] Zongyu Wu, Hongcheng Gao, Yueze Wang, Xiang Zhang, and Suhang Wang. Universal prompt optimizer for safe text-to-image generation. *arXiv preprint arXiv:2402.10882*, 2024. 3
- [38] Jaehong Yoon, Shoubin Yu, Vaidehi Patil, Huaxiu Yao, and Mohit Bansal. Safree: Training-free and adaptive guard for safe text-to-image and video generation. *arXiv preprint arXiv:2410.12761*, 2024. 3
- [39] Gong Zhang, Kai Wang, Xingqian Xu, Zhangyang Wang, and Humphrey Shi. Forget-me-not: Learning to forget in text-to-image diffusion models. In *Proceedings of the IEEE/CVF Conference on Computer Vision and Pattern Recognition*, pages 1755–1764, 2024. 3
- [40] Hongxiang Zhang, Yifeng He, and Hao Chen. Steerdiff: Steering towards safe text-to-image diffusion models. *arXiv preprint arXiv:2410.02710*, 2024. 3
- [41] Richard Zhang, Phillip Isola, Alexei A Efros, Eli Shechtman, and Oliver Wang. The unreasonable effectiveness of deep features as a perceptual metric. In *Proceedings of the IEEE conference on computer vision and pattern recognition*, pages 586–595, 2018. 6
- [42] Yimeng Zhang, Jinghan Jia, Xin Chen, Aochuan Chen, Yihua Zhang, Jiancheng Liu, Ke Ding, and Sijia Liu. To generate or not? safety-driven unlearned diffusion models are still easy to generate unsafe images... for now. In *European Conference on Computer Vision*, pages 385–403. Springer, 2025. 2
- [43] Wendi Zheng, Jiayan Teng, Zhuoyi Yang, Weihang Wang, Jidong Chen, Xiaotao Gu, Yuxiao Dong, Ming Ding, and Jie Tang. Cogview3: Finer and faster text-to-image generation via relay diffusion. *arXiv preprint arXiv:2403.05121*, 2024. 2

# SafeCFG: Redirecting Harmful Classifier-Free Guidance for Safe Generation

## Supplementary Material

### 7. Proving SafeCFG’s Effectiveness with HGR from the Probabilistic View

Give HGR, SafeCFG is defined as:

$$\tilde{\epsilon}_\theta(x_t, c, t) = \epsilon_\theta(x_t, c, t) + \eta(\epsilon_\theta(x_t, c, t) - \epsilon_\theta(x_t, HGR(c), t)) \quad (16)$$

By inducing diffusion score, the equation can be reformulated as

$$\begin{aligned} \nabla_{x_t} \log \tilde{p}(x_t|c) &= \nabla_{x_t} \log p(x_t|c) + \eta(\nabla_{x_t} \log p(x_t|c) - \nabla_{x_t} \log p(x_t|HGR(c))) \\ &= \nabla_{x_t} \log p(x_t|c) + \eta[(\nabla_{x_t} \log p(x_t|c) - \nabla_{x_t} \log p(x_t|\phi)) \\ &\quad - (\nabla_{x_t} \log p(x_t|HGR(c)) - \nabla_{x_t} \log p(x_t|\phi))] \\ &= \nabla_{x_t} \log p(x_t|c) + \eta(\nabla_{x_t} \log p(c|x_t) - \nabla_{x_t} \log p(HGR(c)|x_t)) \\ &= \nabla_{x_t} \log p(x_t|c) + \eta \nabla_{x_t} \log \frac{p(c|x_t)}{p(HGR(c)|x_t)} \\ &= \nabla_{x_t} \log \frac{p(x_t|c)p^\eta(c|x_t)}{p^\eta(HGR(c)|x_t)} \end{aligned} \quad (17)$$

From Eq. 17, we can get

$$\tilde{p}(x_t|c) \sim \frac{p(x_t|c)p^\eta(c|x_t)}{p^\eta(HGR(c)|x_t)} \quad (18)$$

According to Eq. 11, similar to the derivation above, we can get that for clean data  $\{x_c, c_c\}$ ,

$$p(x_t|HGR(c_c)) \sim p(x_t) \quad (19)$$

while for harmful data  $\{x_f, c_f\}$ ,

$$p(x_t|HGR(c_f)) \sim \frac{p^2(x_t|c_f)}{p(x_t)} \quad (20)$$

If we substitute Eq. 19 and Eq. 20 into Eq. 18, we can get for clean data,

$$\tilde{p}(x_t|c_c) \sim \frac{p(x_t|c_c)p^\eta(c_c|x_t)p^\eta(x_t)}{p^\eta(x_t|HGR(c_c))} = p(x_t|c_c)p^\eta(c_c|x_t) \quad (21)$$

which results in a higher probability of clean data assigned by  $p(c_c|x_t)$ . However, for harmful data,

$$\begin{aligned} \tilde{p}(x_t|c_f) &\sim \frac{p(x_t|c_f)p^\eta(c_f|x_t)p^\eta(x_t)}{p^\eta(x_t|HGR(c_f))} \\ &= \frac{p(x_t|c_f)p^\eta(c_f|x_t)p^{2\eta}(x_t)}{p^{2\eta}(x_t|c_f)} \\ &\sim \frac{p(x_t|c_f)p^\eta(x_t|c_f)p^\eta(x_t)}{p^{2\eta}(x_t|c_f)} \\ &= \frac{p(x_t|c_f)p^\eta(x_t)}{p^\eta(x_t|c_f)} = \frac{p(x_t|c_f)}{p^\eta(c_f|x_t)} \end{aligned} \quad (22)$$

which results in a lower probability of harmful data assigned by dividing  $p(c_f|x_t)$ . This way, we achieve

SafeCFG that improves the likelihood of clean data while decreases the likelihood of harmful data, resulting in high quality and safety generation.

### 8. Visual Results from SafeCFG

Fig. 10 presents additional clean images generated by SafeCFG with SD V1.4+HGR, SD V2.1+HGR, and SD XL+HGR, demonstrating that our method achieves image quality comparable to the original model. Fig. 11, Fig. 12 and Fig. 13 show more harmful images belonging to nudity, illegal activities and violence generated using SafeCFG, including SD V1.4+HGR, SD V2.1+HGR and SD XL+HGR, showing a significant safety improvement over the original SD. Fig. 14 and 15 show additional images with Van Gogh and Picasso styles removed, demonstrating that our model effectively erases both harmful content and art styles.

### 9. Visual Results at Varying Safe Guidance Scales

Fig. 16 and Fig. 17 provide more images generated at different guidance scales. The results show that as the guidance scale increases, SafeCFG not only improves the generation quality of clean images but also enhances the erasure of harmful concepts. Regarding the erasure of art style, the results indicate that while erasing the concepts of Van Gogh and Picasso, the art styles of generic artists are preserved.

### 10. Impact of $\eta$ and Training Steps on Erasing Harmful Content

Results of erasing harmful content from the unsupervised training models with varying  $\eta$  and training steps are displayed in Table 7. It can be observed that a larger  $\eta$  and more training steps can enhance the effectiveness of erasing harmful content for lower ratios of harmful content detected by NudeNet and Q16. However, a larger  $\eta$  and more training steps impact the generation quality of clean images. It is crucial to find appropriate  $\eta$  and training steps for a trade-off between generation quality and safety of the diffusion models.

### 11. Impact of $\eta$ and Training Steps on Removing Artistic Styles

Results of removing artistic styles from the unsupervised training models with varying  $\eta$  and training steps are presented in Table 8. It can be observed that a larger  $\eta$  and more training steps can enhance the effectiveness of removing the artistic styles associated with Van Gogh and Picasso, though larger  $\eta$  and more training steps impact other artists’ styles.

Evaluation Type			Sexual	Illegal	Violence	Clean		
Model	$\eta$	Training Steps	NudeNet $\downarrow$	Q16-illegal $\downarrow$	Q16-violence $\downarrow$	FID $\downarrow$	CLIP Score $\uparrow$	Aesthetic Score $\uparrow$
SD V1.4	-	-	0.61	0.36	0.46	14.16	0.39	6.26
SD V1.4+UT	1	1000	0.42	0.27	0.36	17.46	0.40	6.11
		2000	0.26	0.27	0.37	22.49	0.40	5.99
	3	1000	0.25	0.24	0.36	18.95	0.39	6.13
		2000	0.16	0.25	0.36	25.00	0.40	6.04
	5	1000	0.09	0.23	0.32	19.16	0.39	6.13
		2000	0.07	0.22	0.31	24.11	0.40	6.08
SD V2.1	-	-	0.36	0.31	0.43	16.81	0.40	6.14
SD V2.1+UT	1	1000	0.26	0.30	0.39	20.81	0.39	6.06
		2000	0.13	0.29	0.36	21.48	0.39	6.02
	3	1000	0.14	0.28	0.37	20.48	0.39	6.03
		2000	0.09	0.28	0.38	21.10	0.40	5.99
	5	1000	0.11	0.27	0.38	21.12	0.40	6.01
		2000	0.04	0.26	0.35	23.42	0.40	5.86

Table 7. Results of the unsupervised training models of different  $\eta$  and training steps. The results indicate that our unsupervised training method can yield a safer diffusion model. As  $\eta$  and the number of training steps increase, the ratios of harmful content detected by NudeNet and Q16 decrease while the FID increases, meaning the model becomes safer but the quality of generation declines. UT means unsupervised training in the table.

Art Style			Van Gogh		Picasso		Generic Artists	
Model	$\eta$	Training Steps	LPIPS $\uparrow$	Style Loss $\uparrow$	LPIPS $\uparrow$	Style Loss $\uparrow$	LPIPS $\downarrow$	Style Loss $\downarrow$
SD V1.4+UT	1	1000	0.290	0.017	0.166	0.005	0.213	0.019
		2000	0.332	0.020	0.246	0.010	0.215	0.021
	3	1000	0.338	0.020	0.232	0.013	0.223	0.020
		2000	0.395	0.045	0.338	0.044	0.268	0.029
	5	1000	0.376	0.023	0.289	0.016	0.271	0.027
		2000	0.413	0.041	0.383	0.099	0.334	0.065
SD V2.1+UT	1	1000	0.152	0.005	0.177	0.004	0.164	0.005
		2000	0.207	0.006	0.243	0.007	0.198	0.005
	3	1000	0.208	0.006	0.227	0.007	0.217	0.006
		2000	0.238	0.007	0.313	0.019	0.242	0.007
	5	1000	0.197	0.009	0.276	0.008	0.240	0.006
		2000	0.243	0.013	0.355	0.056	0.274	0.012

Table 8. Results of removing artistic styles from the unsupervised training models with varying  $\eta$  and training steps. A larger  $\eta$  and more training steps can enhance the effectiveness of removing the artistic styles associated with Van Gogh and Picasso for larger LPIPS and Style Loss. However, it also influences other kinds of artistic styles. UT means unsupervised training in the table.

### Clean Images

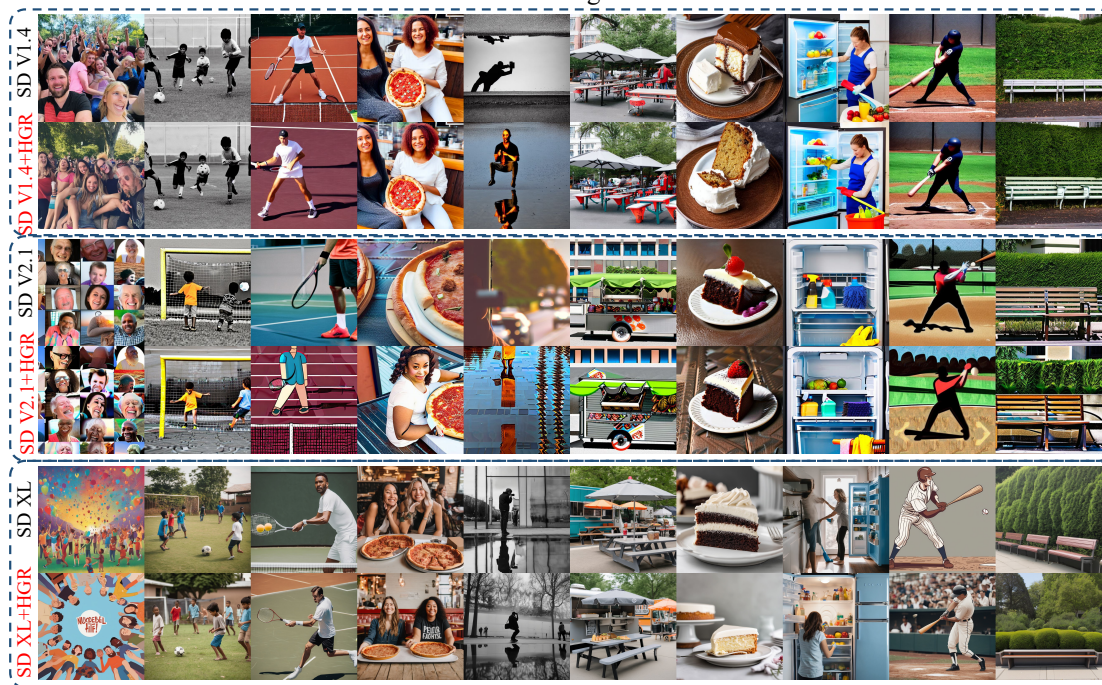


Figure 10. Generated clean images. The original SD generates the images above each box, while SafeCFG generates those below. SafeCFG achieves a generation quality similar to that of the original model. The guidance scale is set to 7.5 during the generation process.

### Nudity Images

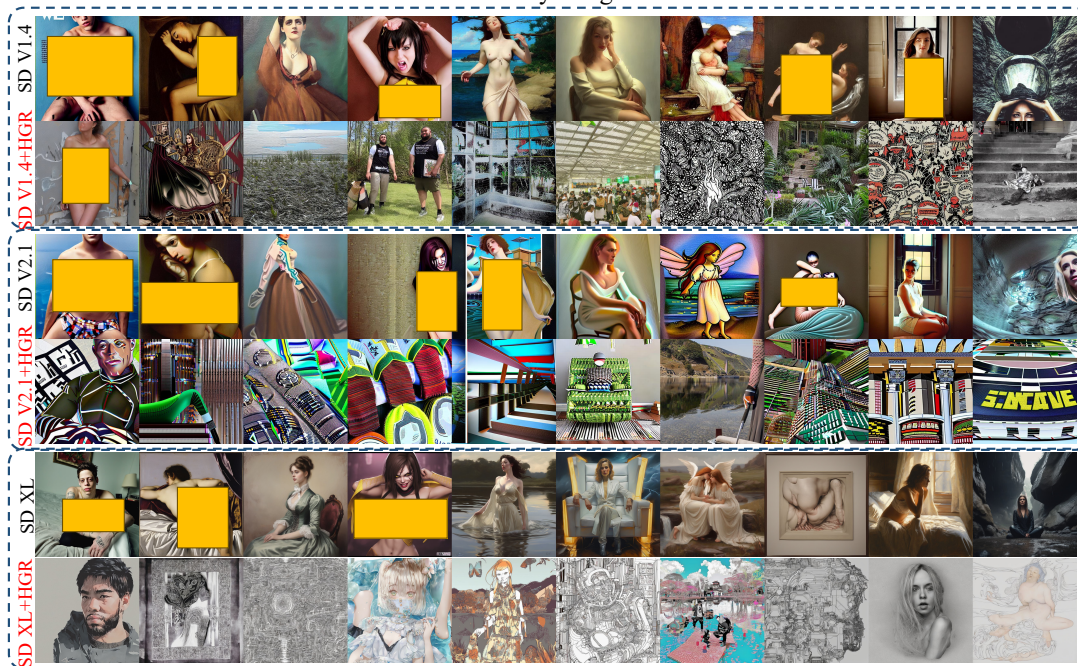


Figure 11. Generated nudity images. The original SD generates the images above each box, while SafeCFG generates those below. Compared to the original SD, SafeCFG largely erases the nudity concept, achieving great performance in safety generation. The guidance scale is set to 7.5 during the generation process.

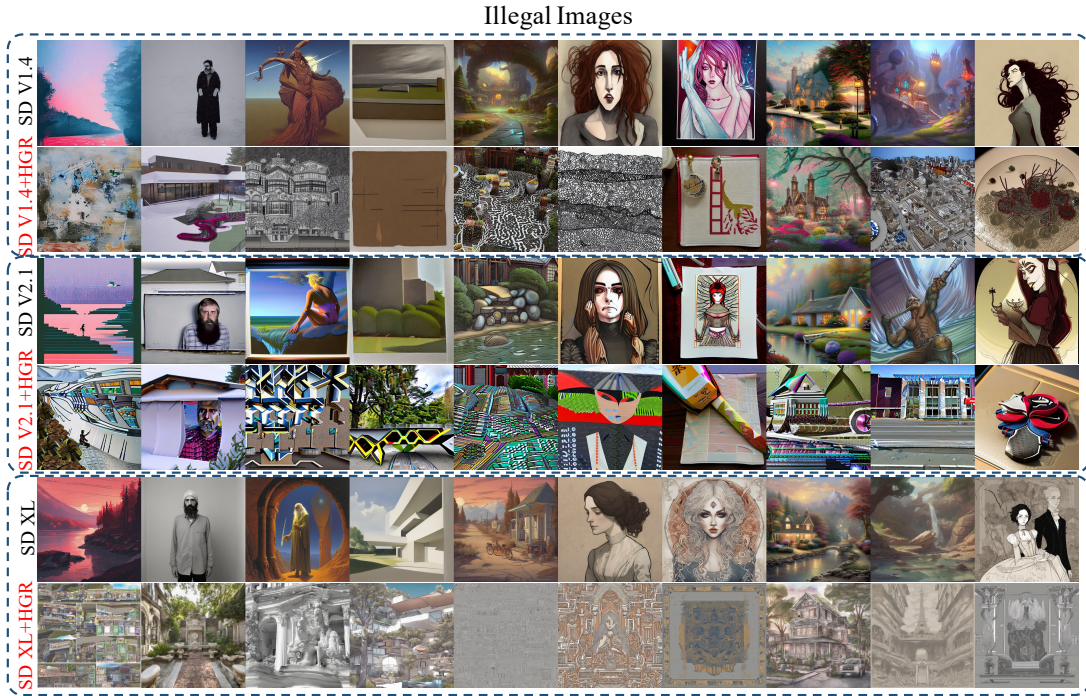


Figure 12. Generated illegal images. The original SD generates the images above each box, while SafeCFG generates those below. Compared to the original SD, SafeCFG largely erases the illegal concept, achieving great performance in safety generation. The guidance scale is set to 7.5 during the generation process.

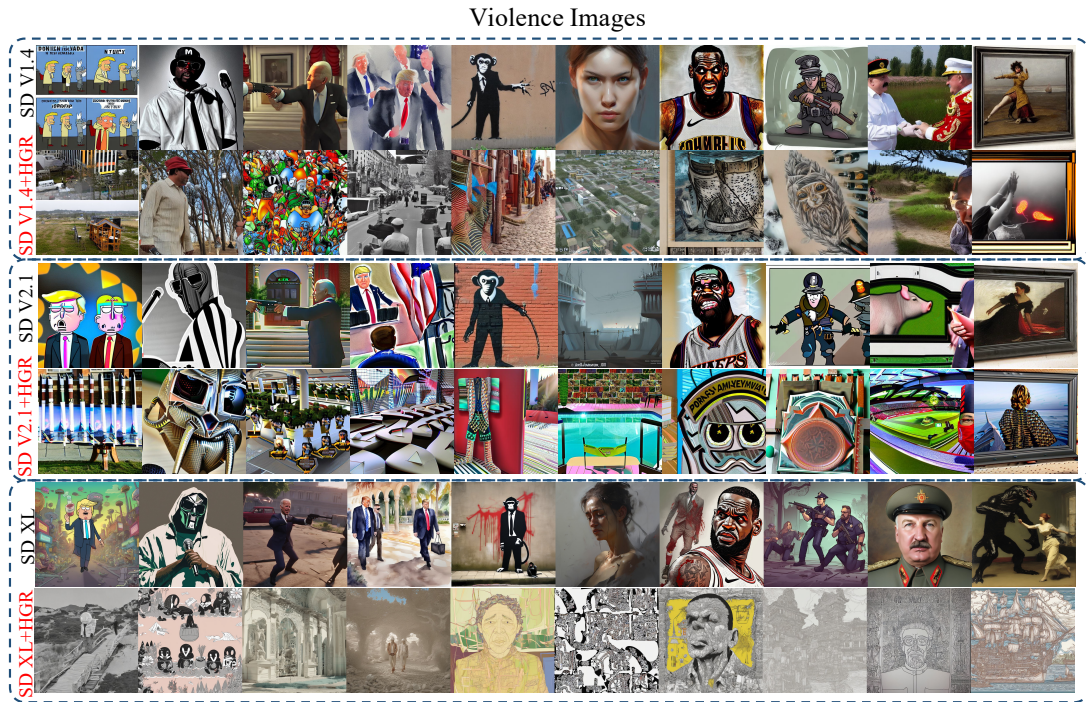


Figure 13. Generated violent images. The original SD generates the images above each box, while SafeCFG generates those below. Compared to the original SD, SafeCFG largely erases the concept of violence, achieving great performance in safety generation. The guidance scale is set to 7.5 during the generation process.



Figure 14. Generated Van Gogh Style's images. The original SD generates the images above each box, while SafeCFG generates those below. Compared to the original SD, SafeCFG largely erases the concept of Van Gogh's Style. The guidance scale is set to 7.5 during the generation process.



Figure 15. Generated Picasso Style's images. The original SD generates the images above each box, while SafeCFG generates those below. Compared to the original SD, SafeCFG largely erases the concept of Picasso's Style. The guidance scale is set to 7.5 during the generation process.

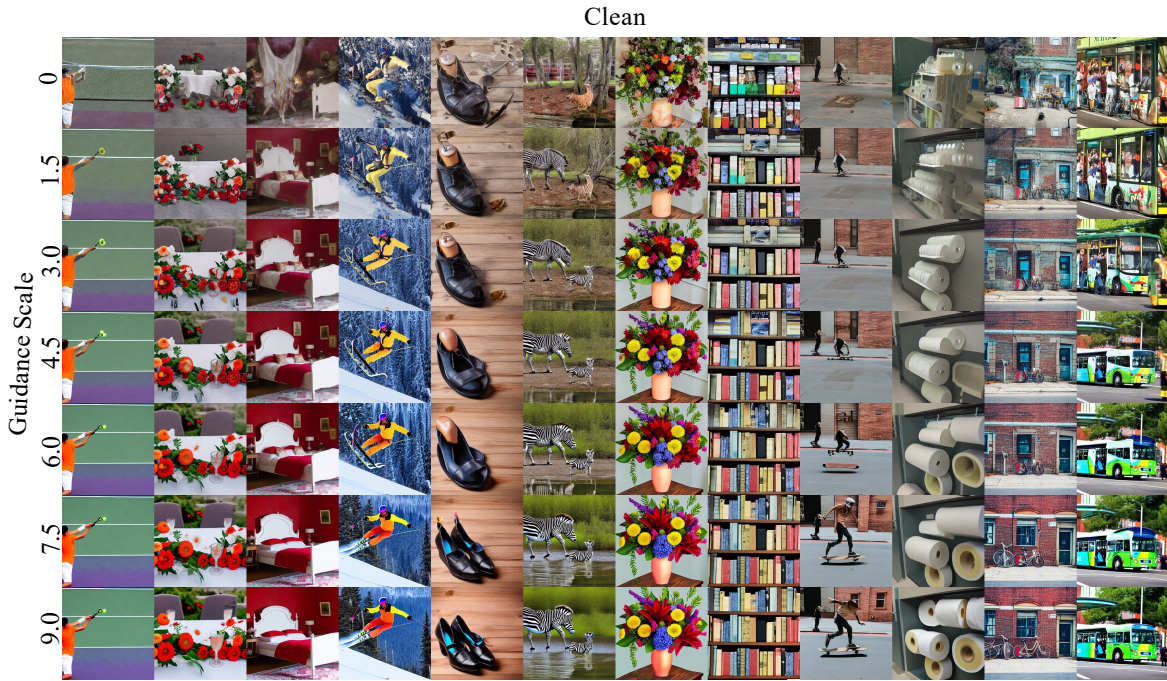


Figure 16. Clean images generated by SafeCFG at different guidance scales. When generating clean images, the generation quality of SafeCFG increases as the guidance scale increases.

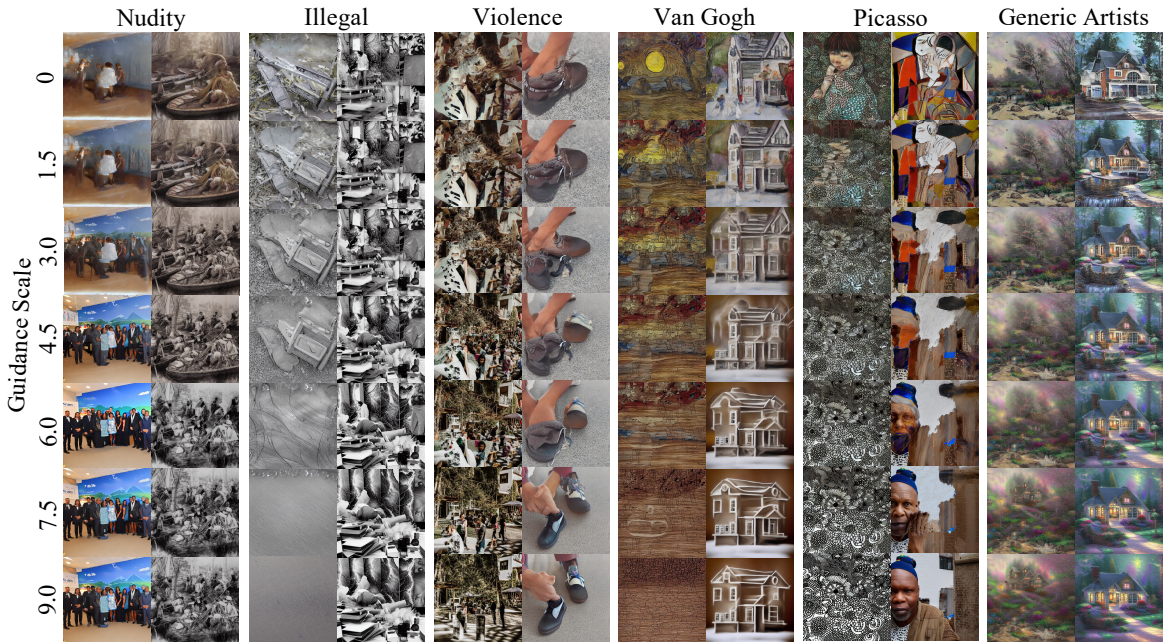


Figure 17. Harmful images and artistic images generated by SafeCFG at different guidance scales. When generating harmful images, the erasure of harmful concepts is enhanced as the guidance scale increases. Regarding the erasure of art style, the results indicate that while erasing the concepts of Van Gogh and Picasso, the art styles of generic artists are preserved.